ITC 2/55

Information Technology and Control
Vol. 55 / No. 2/ 2026
pp. 880-900
DOI 10.5755/j01.itc.55.2.43113

Health Assessment of Cigarette Factory Drying Machine Equipment by Integrating SimCLR Framework and Wavelet Transform

Received 2025/10/15 | Accepted after revision 2026/02/12

HOW TO CITE: Wang, M., Xu, Y. (2026) Health Assessment of Cigarette Factory Drying Machine Equipment by Integrating SimCLR Framework and Wavelet Transform. *Information Technology and Control*, 55(2), 880-900. https://doi.org/10.5755/j01.itc.55.2.43113

Health Assessment of Cigarette Factory Drying Machine Equipment by Integrating SimCLR Framework and Wavelet Transform

Meng Wang*

College of Information Engineering, Lanzhou Petrochemical University of Vocational Technology, Lanzhou 730060, China

Yibo Xu

Gansu Tobacco Industrial Co., Ltd. Lanzhou Cigarette Factory, Lanzhou 730050, China

Corresponding author: wangmeng202507@163.com

In the process of cigarette production, the drying machine, as the core equipment, has low operation and maintenance efficiency and lacks correlation analysis between macro health status and micro fault roots, making it difficult to meet the needs of intelligent manufacturing. To address this challenge, the study aims to construct a dual-layer intelligent health assessment framework that combines macroscopic overall health status assessment of equipment with microscopic key component fault diagnosis. At the macro level, a dynamic health assessment model based on game theory combined with weighting is proposed, which optimizes the subjective weights of the fuzzy analytic hierarchy process and the objective weights of the entropy weight method through Nash equilibrium. At the micro level, a simple framework for unsupervised fault diagnosis of key components, such as rolling bearings, is constructed by integrating continuous wavelet transform and representation contrastive learning. Comparative learning is used to extract strong, robust fault features from unlabeled data. The experimental results showed that the mean absolute error of the macro evaluation model during the state transition stage was only 3.15, and the average evaluation accuracy reached 97.2%, which was significantly better than the traditional weighting model. The accuracy of the micro diagnostic model remained at 90.2% in strong noise environments, and the missed diagnosis rate in variable load testing was less than 2.7%. This dual-layer framework effectively achieves a precise closed-loop from overall monitoring to component diagnosis, providing a theoretically valuable solution for predictive maintenance and intelligent operation of complex industrial equipment.

KEYWORDS: Tobacco dryer; Health assessment; Combination weighting; SimCLR; Fault diagnosis; Wavelet transform; Self-supervised learning

1. Overview

Under the wave of Industry 4.0 and smart manufacturing, the global manufacturing industry is undergoing a profound digital transformation. Its core is to build highly automated and information-based smart factories through cutting-edge technologies such as the Internet of Things (IoT), big data, and artificial intelligence. In this context, device prediction and health management have become key technologies for the core competitiveness of enterprises [19, 5, 12]. In industries with precise processes, such as cigarette production, fluctuations in any link of the production chain can trigger a chain reaction. Among them, the tobacco dryer, as the core equipment in the cigarette production process, has the function of accurately controlling key process parameters such as moisture content and temperature of the cigarette, and its health status directly determines the quality of the final product. However, the tobacco dryer itself is a complex system that integrates mechanical transmission, thermodynamics, and electrical control, with variable operating conditions and numerous potential failure modes [22, 21, 13]. The traditional operation and maintenance mode mainly includes regular maintenance with fixed cycles and post-maintenance after faults occur. The former has limitations such as over-maintenance and under-maintenance, which can easily waste the life of healthy components and cannot effectively prevent sudden failures [16]. The latter has the defect of delayed response, which can interrupt the entire production plan in case of the unexpected shutdown of core components [11, 1]. Therefore, the existing model cannot satisfy the high demands of the modern cigarette industry for intelligent equipment operation and maintenance. There is an urgent need to build a new intelligent evaluation system that can accurately assess the overall health status of equipment and diagnose potential faults in key components.

In complex system health assessment and decision-making, the combination weighting and multi-criteria decision-making methods that integrate subjective and objective information has become a research hotspot. A single performance indicator is difficult to precisely assess the health status of the tool magazine robotic arm, and small sample data makes fault prediction difficult. To this end, Li et al. [9] proposed a health assessment model that integrates Fuzzy Comprehensive Evaluation (FCE) and a combined weighting method, and constructed a fault prediction method built on PSO. The proposed evaluation method integrated subjective and objective factors, effectively improving the reliability of the evaluation. Meanwhile, the prediction accuracy has also been verified [9]. Zhang et al. [28] developed a new control model based on the Entropy Weight Method (EWM) to deal with the limitations of traditional schedule management methods in tobacco re-roasting plant renovation projects. It was more objective and effective than the traditional Gantt chart method, had stronger operability in project schedule management, and could determine a more reasonable and accurate total project duration [28]. Więckowski et al. [25] proposed a decision-making method that combines artificial neural network modeling and EWM approximation ideal solution to address the complex process parameters in Ti-6Al-4V alloy wire cutting machining. This method could effectively determine a set of optimal process parameter combinations, providing a more convenient solution for parameter selection in complex machining processes [25]. Xu et al. [27] constructed a 4D evaluation system to address the frequent occurrence and insufficient research on flood risks, and used a combination of network Analytic Hierarchy Process (AHP), EWM weighting, and approximate ideal solution for comprehensive evaluation. This method was feasible and effective, providing a decision-making basis for the scientific management of regional flood risks [27]. In the event of a sudden public health emergency, the location decision of emergency medical supplies distribution centers is full of uncertainty. Liu et al. [11] proposed a novel multi-criteria decision-making method that integrates cumulative prospect theory, neighbor avoidance effect, fuzzy network analysis, and EWM. The effectiveness of the innovative model has been demonstrated through case analysis and sensitivity analysis [11].

At the micro fault diagnosis level of key components, self-supervised methods built on deep learning have great potential. Wang et al. [24] proposed a prototype-based Supervised Contrastive Learning (SCL) method to address low performance in tire defect detection. This method utilized an SCL framework to aggregate features from similar samples to generate class prototypes, which were then used to correct labels for training reliable networks. Even with a high proportion of noise, this method still had strong robustness [24]. Zhang et al. [30] designed a Fault Diagnosis Method (FDM) built on contrastive learning to address the challenges of limited labeled samples and imbalanced categories in rotating machinery fault diagnosis. This method utilized unlabeled data by designing a feature fusion network and employed a dynamic weighted loss function to mitigate the impact of class imbalance. This method could achieve higher diagnostic accuracy under conditions of limited labels and imbalanced data [30]. In response to the challenge of overfitting in bearing fault diagnosis due to the scarcity of labeled data, Zhang et al. [29] proposed a semi-SCL method that integrates multi-objective contrastive learning and multi-scale attention. The diagnostic performance was superior to other similar methods under limited labeled samples [29]. Wu et al. [26] put forth a novel FDM built on the premise that nominal operating state data is easier to obtain, in response to the challenge of limited performance of supervision models in health management caused by scarce fault data. This method used a probability distribution generalization strategy and a comparative transformation optimization method to pre-train and fine-tune the model. This model effectively improved the classification accuracy under different operating conditions [26]. Hu et al. [4] proposed a Self-Supervised Learning (SSL) framework that integrates cross-instance and cross-time approaches to address the issue of overfitting in intelligent FDMs caused by insufficient annotated data in practical applications. This method extracted features by transforming consistency learning and temporal relationship matching tasks, showing that the proposed framework outperforms other supervised and semi-supervised methods [4]. In the broader field of intelligent monitoring and health management, research based on the IoT and advanced deep learning architectures has made significant progress in complex systems. Mohammed et al. [14] proposed an IoT and edge cloud network architecture driven by federated learning, which effectively improves the navigation accuracy and data security of intelligent wheelchair systems through real-time data collection and processing [14]. Lakhan et al. [8] constructed a digital healthcare framework based on deep federated learning, which achieved 99% accuracy in disease prediction for disabled patients by integrating medical IoT sensor data. This framework significantly reduced system energy consumption and response time [8].

In summary, although deep learning is widely used in the industrial field, it still faces challenges in handling multi-source heterogeneous data and privacy protection. In the fields of healthcare and the IoT, research has explored edge cloud networks and digital healthcare frameworks based on federated learning. However, in specific industrial scenarios such as cigarette factory dryers, existing research mostly focuses on single-fault diagnosis or independent health evaluation, lacking a unified framework for effectively integrating macro indicators with micro signals. At the same time, decision-making methods based on combination weighting are difficult to diagnose the root cause of specific component failures in depth, while diagnostic methods centered on deep learning often ignore the overall macro operating background of the equipment. In addition, there is a common problem of label data scarcity in industrial sites, which limits the application of supervised learning models. A DIHAF that integrates macro health status assessment and micro fault diagnosis has been proposed to address such issues. At present, there are few studies that combine macro level comprehensive health assessment with micro level Unsupervised Fault Diagnosis (UFD) to construct a two-layer evaluation framework suitable for complex equipment such as Cigarette Factory Drying Machines (CFDMs). A unique dual-layer execution framework has been proposed to address the aforementioned shortcomings. At the macro level, this paper does not simply superimpose weights but introduces a game theory combination weight mechanism. This paper dynamically balances the conflict between expert experience (Fuzzy Analytic Hierarchy Process, FAHP) and objective data volatility (EWM) by finding Nash equilibrium points, thereby overcoming the subjectivity or sensitivity of a single weight to data noise. At the micro level, in response to the challenge of unlabeled data in industrial sites, an innovative self-supervised diagnostic path combining Continuous Wavelet Transform (CWT) and Simple Framework for Contrastive Learning of Representation (SimCLR) has been constructed. This method does not rely on manual labels but maximizes the feature consistency before and after time-frequency graph transformation, forcing the model to autonomously learn robust fault representations from unlabeled data, thereby achieving accurate diagnosis in strong noise and variable operating conditions. The contributions of the research are as follows: 1. An evaluation system that combines macroscopic health status assessment and microscopic fault diagnosis is innovatively proposed to achieve a comprehensive perception of the dryer from the whole to the part. 2. Game theory is introduced to solve the conflict between subjective weights of FAHP and objective weights of EWM. By finding the Nash equilibrium point to obtain the optimal combination weight, the objectivity of the evaluation is improved. 3. The combination of CWT and SimCLR effectively uses data enhancement and time-frequency characteristics to solve the problem of bearing fault diagnosis in label-free and strong noise environments.

Section 2 explains the method of the binary evaluation framework, including the derivation of the macro-evaluation model and the micro-diagnosis algorithm. Section 3 validates the effectiveness of the proposed method through actual operational data and standard datasets. Section 4 discusses the underlying mechanisms and application value of the experimental results. Section 5 summarizes the entire text and looks forward to future research directions.

2. Methodologies

To achieve dual-layer health assessment of CFDM equipment, this study first introduces a dynamic assessment model for quantifying the macroscopic health status of the equipment. This model integrates FAHP, EWM, and game theory combination weighting. Secondly, this study develops a UFD method for key component rolling bearings. This method innovatively combines CWT and the SimCLR SSL framework.

2.1. HSA of Tobacco Dryer Equipment Based on FAHP and EWM

To achieve comprehensive coverage from overall status monitoring to local fault tracing in the health assessment of CFDM equipment, this study proposes an innovative Dual-layer Intelligent Health Assessment Framework (DIHAF). Macroscopically, this study constructs a Health Status Assessment (HSA) model based on the combination of FAHP and EWM weights and FCE. At the micro level, this paper constructs a UFD method that integrates CWT and representation contrastive learning using the SimCLR framework to address challenges such as strong subjectivity in evaluation and missing fault data labels in actual industrial scenarios. Considering the low accuracy of traditional expert judgment methods and the inability of the fixed weight system used to reflect data dynamics, this study constructs an advanced HSA model for tobacco dryer equipment. The evaluation process is shown in Figure 1. This model integrates FAHP subjective weights, EWM objective weights, and a combination of game theory weighting methods. Firstly, the model uses FAHP and EWM to obtain subjective and objective weights. Then, game theory is introduced to optimize the combination of these two heterogeneous weights. Finally, the obtained combined weights are applied to FCE to achieve an accurate assessment of the health status of the equipment.

The basis of the evaluation model is to accurately quantify the operating status of each component of the equipment. This study mainly starts with the concept of degradation and measures the degree of deviation between the current state of the component and its ideal health state. The degradation degree x_i' of components under different data collection conditions is calculated using a differentiated approach. When the component can obtain real-time operating parameters, the calculation of its degradation degree x_i' is shown in Equation (1) [15].

$$x_i' = \begin{cases} \dfrac{x_i - x_{i0}}{max_i - x_{i0}}, & x_i > x_{i0} \\ 0, & x_i = x_{i0} \\ \dfrac{x_{i0} - x_i}{x_{i0} - min_i}, & x_i < x_{i0} \end{cases} . \tag{1}$$

In Equation (1), x_i is the real-time operating parameter of the component, x_{i0} is the standard reference value of the parameter, max_i is the maximum threshold allowed by the parameter, and min_i is the minimum threshold allowed by the parameter. This formula quantifies the degree to which a component deviates from a healthy state by comparing real-time parameters with standard parameters and thresholds. For components that cannot directly obtain real-time operational data but have a clear fixed lifecycle, their degradation degree x_i' is estimated based on the actual operating time, as expressed in Equation (2).

Figure 1

The evaluation process of the health assessment model for tobacco dryer equipment.

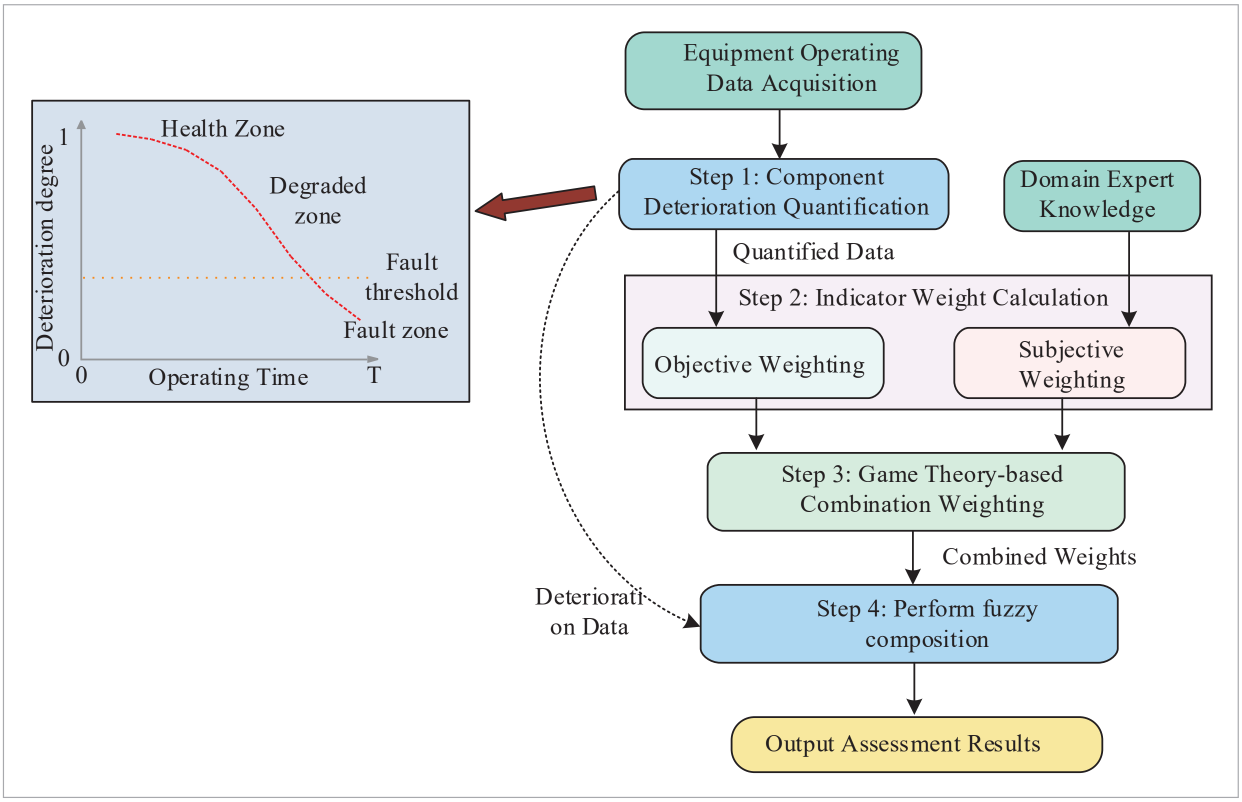

$$x_i' = \begin{cases} t_a / T, & t_a < T \\ 1, & t_a \geq T \end{cases}. \tag{2}$$

In Equation (2), t_a is the actual operating time of the component, and T is the rated life cycle of the component design. When the running time does not reach the rated life cycle, the degradation degree increases linearly with the running time. When the running time reaches or exceeds the rated life cycle, the degradation degree is judged as 1, which means that the component is considered to be approaching or entering a fault state. In Figure 1, the degradation process of a component from a healthy state to a faulty state can be visually presented through a degradation curve. The traditional AHP method requires experts to provide accurate judgment scales, but this is often difficult to achieve when facing complex systems, and it ignores the fuzziness and uncertainty in the judgment process. To address this issue, this study uses FAHP to obtain subjective weights, as shown in Figure 2.

In Figure 2, FAHP calculates subjective weights through four steps: constructing a fuzzy judgment matrix, calculating fuzzy weights, defuzzification, and normalization processing. The subjective weight vector representation of all evaluation indicators is shown in Equation (3).

$$W_s = (w_{s1}^*, w_{s2}^*, \ldots, w_{st}^*). \tag{3}$$

In Equation (3), w_s^* represents the subjective weight of each evaluation index after normalization. To compensate for the one-sidedness of subjective weighting, this study further introduces EWM to calculate objective weights. EWM relies entirely on the information in the data. The smaller information entropy of the indicator data indicates a greater variation degree of the indicator value, more information it provides, and a higher weight it should occupy in the comprehensive evaluation. The calculation flow of EWM is shown in Figure 3.

Figure 2

Flowchart for FAHP to obtain subjective weights.

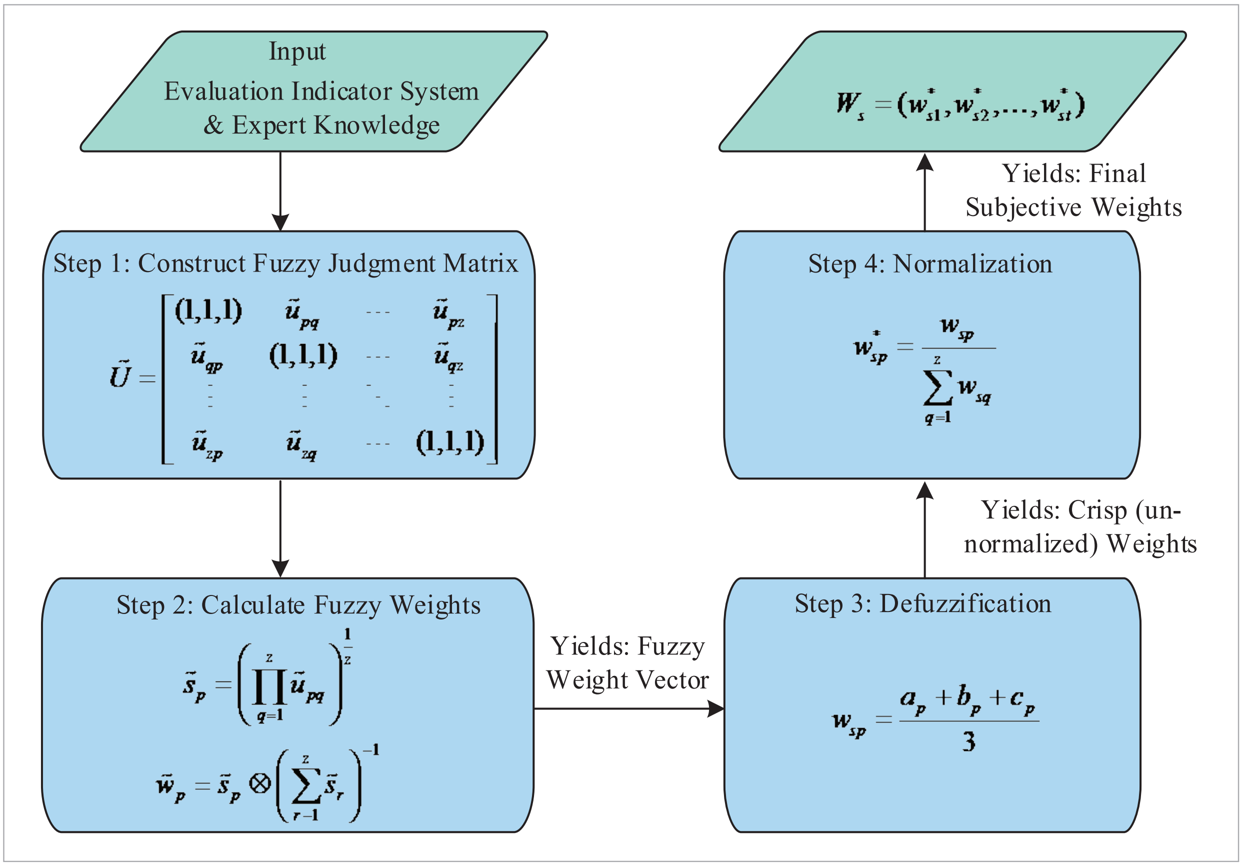

Figure 3

The calculation process of EWM.

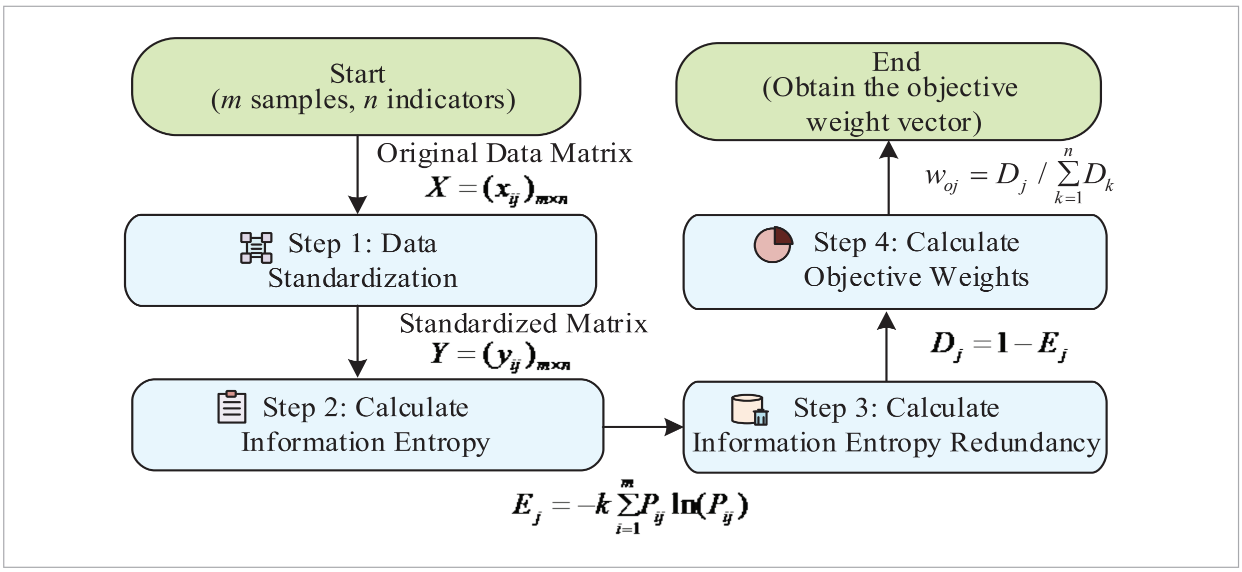

In Figure 3, the process of calculating objective weights using EWM consists of four steps. Firstly, data standardization is carried out. When there are A samples to be evaluated and A evaluation indicators, the original data matrix is first constructed, and the expression is shown in Equation (4).

$$X = (x_{ij})_{m \times n} . \tag{4}$$

In Equation (4), x_{ij} is the raw data of sample i under indicator j, among which, i=1,2,...,m, j=1,2,...,n. To eliminate the differences in metrics between different indicators, standardization operations are carried out on the raw data, resulting in a standardized matrix as shown in Equation (5).

$$Y = (y_{ij})_{m \times n} . \tag{5}$$

In Equation (5), Y is the standardized matrix. y_{ij} is the standardized value of x_{ij}, used to eliminate the influence of different indicator dimensions. Subsequently, objective weights are calculated. The objective weight w_{oj} of the j-th indicator is determined by its redundancy D_j, as shown in Equation (6).

$$w_{oj} = \frac{D_j}{\sum_{k=1}^{n} D_k} . \tag{6}$$

Finally, the objective weight vector W_o=(w_{o1},w_{o2},...,w_{on}) is obtained. Thus, subjective weight vector W_s and objective weight vector W_o are obtained. This study introduces game theory to solve the optimal combination of the two and obtains an optimal combination weight W^*. The FCE method is used to calculate the final health status score H of the device, as shown in Figure 4.

In Figure 4, first, it is necessary to establish a set of comments V for five levels of health, good, attention, abnormality, and fault, and input the component degradation degree x' to convert the health status score H_p on a hundred point scale. The next step is to calculate the fuzzy relationship matrix R for the membership degree of each health level. Then, W^* is input and subjected to fuzzy synthesis operation with the

Figure 4

Final health calculation process.

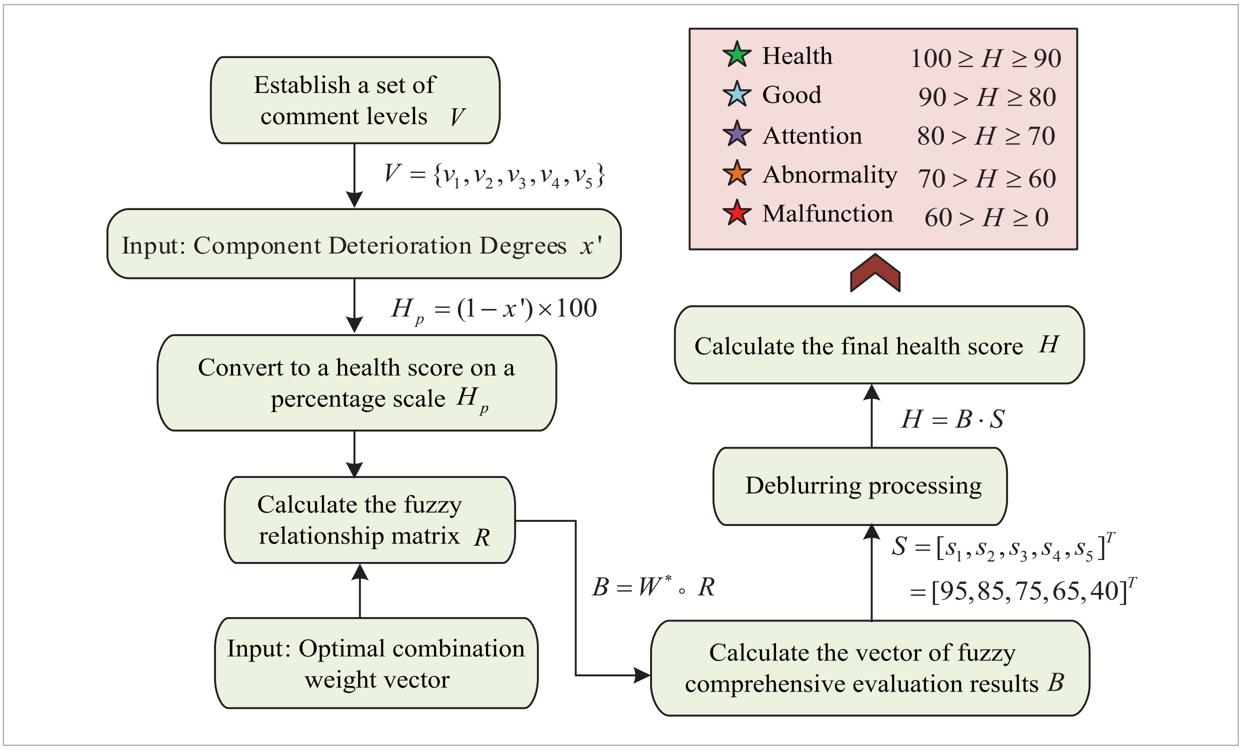

R to obtain the FCE result vector B. Afterwards, a vector containing the standard scores of each health level is introduced for deblurring processing, and the final health status score H of the device is finally calculated. Different health status score intervals correspond to different health statuses.

2.2. UFD Method Integrating Wavelet Transform and SimCLR

After using the HSA model to determine the overall health level of the equipment and tracking changes in status, it will then enter the micro level and use effective FDMs to locate the root cause of specific component failures. The fault diagnosis of rolling bearings in CFDM is crucial for the overall health of the equipment. However, in practical industrial scenarios, problems such as scarce fault samples, missing data labels, and variable operating conditions often occur. Traditional supervised learning models that rely heavily on annotated data are difficult to apply. To handle this challenge, the paper proposes a UFD method based on self-SCL. This method combines CWT and the SimCLR framework, as shown in Figure 5.

In Figure 5, the UFD process that integrates the wavelet transform and the SimCLR framework is mainly divided into three stages. Firstly, in the data processing stage, the original 1D Vibration Signal (1DVS) of

Figure 5

Fault diagnosis process integrating CWT and SimCLR.

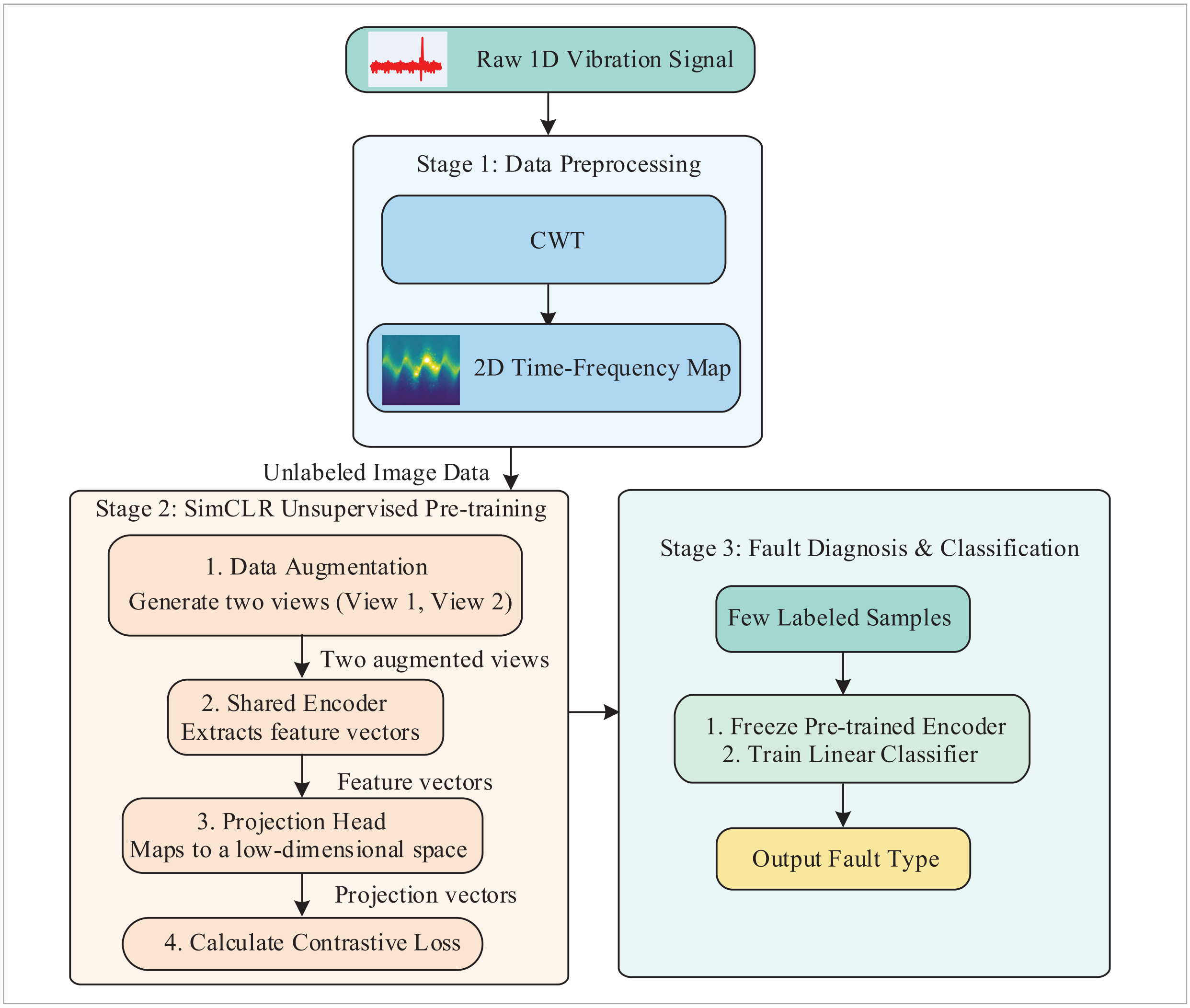

the rolling bearing is transformed into a 2D Time-Frequency (2DTF) map that can simultaneously represent both time-domain and frequency-domain information using CWT. Then, it enters the unsupervised pre-training phase of SimCLR, which first generates two views for each time-frequency graph through data augmentation operations such as random cropping and flipping. The next step is to use a shared encoder to extract the feature vectors of the view, map them to a low-dimensional space through a projection head to obtain the projection vectors, and calculate the contrastive loss to optimize the model. Finally, there is the stage of fault diagnosis and classification, which combines a small number of labeled samples, freezes pre-trained encoder parameters, trains a linear classifier, and then achieves the recognition of rolling bearing fault types. The original vibration signal of rolling bearings is 1D time-series data, and direct analysis is difficult to fully reveal its nonlinear and non-stationary features. To effectively extract fault features, it is necessary to convert 1D signals into 2D representations that can simultaneously represent both time and frequency domain information. Therefore, CWT is chosen in this study to achieve this transformation. Compared to the fixed window of Short-Time Fourier Transform (STFT) and the cross-term interference problem of Wigner-Ville Distribution (WVD), CWT has the characteristics of multi-resolution analysis. The time-frequency window of this method can be adaptively adjusted, with high time resolution in the high-frequency part and high-frequency resolution in the low-frequency part, making it suitable for capturing transient impact signals generated by bearing faults [20, 3]. Wavelet transform mainly achieves multi-scale analysis of signals by scaling operations on the wavelet basis function $\psi(t)$. The wavelet basis function obtained after transformation is given by Equation (7).

$$\psi_{c,d}(t) = \frac{1}{\sqrt{c}}\psi\left(\frac{t-d}{c}\right). \tag{7}$$

In Equation (7), t is a time variable. c represents the scale factor used to control the degree of wavelet scaling. d is a time shift factor responsible for adjusting the position of the wavelet on the time axis. For the temporal vibration signal $r(t)$ that satisfies the square integrability condition, the calculation of its CWT result $H_\psi(c,d)$ is shown in Equation (8).

$$H_\psi(c,d) = \frac{1}{\sqrt{c}}\int_{-\infty}^{\infty} r(t)\psi^*\left(\frac{t-d}{c}\right)dt \tag{8}$$

Considering that bearing fault signals often exhibit transient impact characteristics, this study selects Morlet wavelets that are highly similar to the waveform of the impact signal as the mother wavelet. Morlet wavelets can achieve good localization in both time-frequency domains, thus more effectively extracting fault feature information. By performing a wavelet transform on the original 1DVS samples, each sample will be transformed into a 2DTF map, as shown in Figure 6.

Figure 6(a) shows the original 1DVS, with the horizontal and vertical axes representing time and ampli-

Figure 6
Schematic diagram of wavelet transform operation.

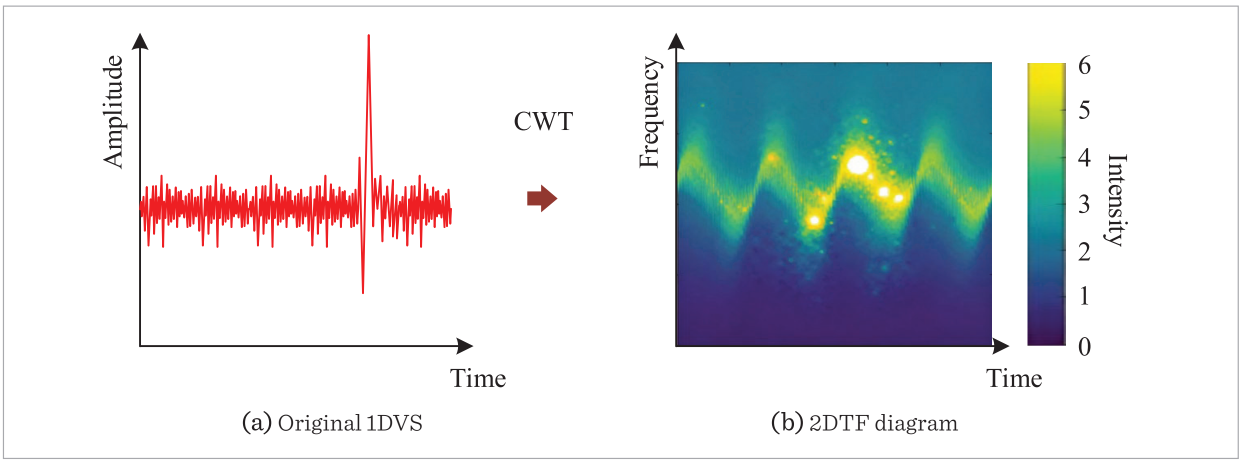

tude. The signal exhibits transient shock characteristics. After CWT, the 2DTF plot in Figure 6(b) still shows the color bar on the right reflecting energy intensity. Due to the excellent localization properties of Morlet wavelets in the time-frequency domain, they are suitable for the transient impact characteristics of bearing faults. Therefore, the converted time-frequency diagram can display the energy distribution of the fault signal at various times and frequencies. Subsequently, the time-frequency diagram is input into SimCLR for fault diagnosis. SimCLR is a simple and efficient contrastive learning framework that learns feature representations by maximizing consistency between different views of the same sample, without the need for any manual labeling [23, 2, 7]. This study utilizes the SimCLR framework for unsupervised pre-training of the wavelet time-frequency maps generated in the previous stage, as shown in Figure 7.

In Figure 7, the SimCLR process mainly includes three key stages: data augmentation, feature encoding and projection, and contrastive loss calculation. The first step is to input a batch of wavelet time-frequency maps, randomly select a sample from the batch, and apply two different random data augmentation transformations to it to generate a pair of correlated views. Two views form a positive sample pair, which is the foundation of contrastive learning. The two enhanced views are then fed into two twin network pipelines with the same structure and shared weights. Each enhanced view maps high-dimensional image data into low-dimensional feature representation vectors through a basic encoder network. Next, the feature vectors are projected onto a latent space more suitable for calculating contrast loss through a projection head composed of a small Multi-Layer Perceptron (MLP), resulting in the final projection vector. Finally, projection vector pairs from the same original sample will be fed into a similarity function to calculate similarity, and the calculated results will be used for comparing the loss calculation. Through this process, the model can learn effective features that can distinguish different fault states. To visually demonstrate the end-to-

Figure 7

SimCLR framework diagram.

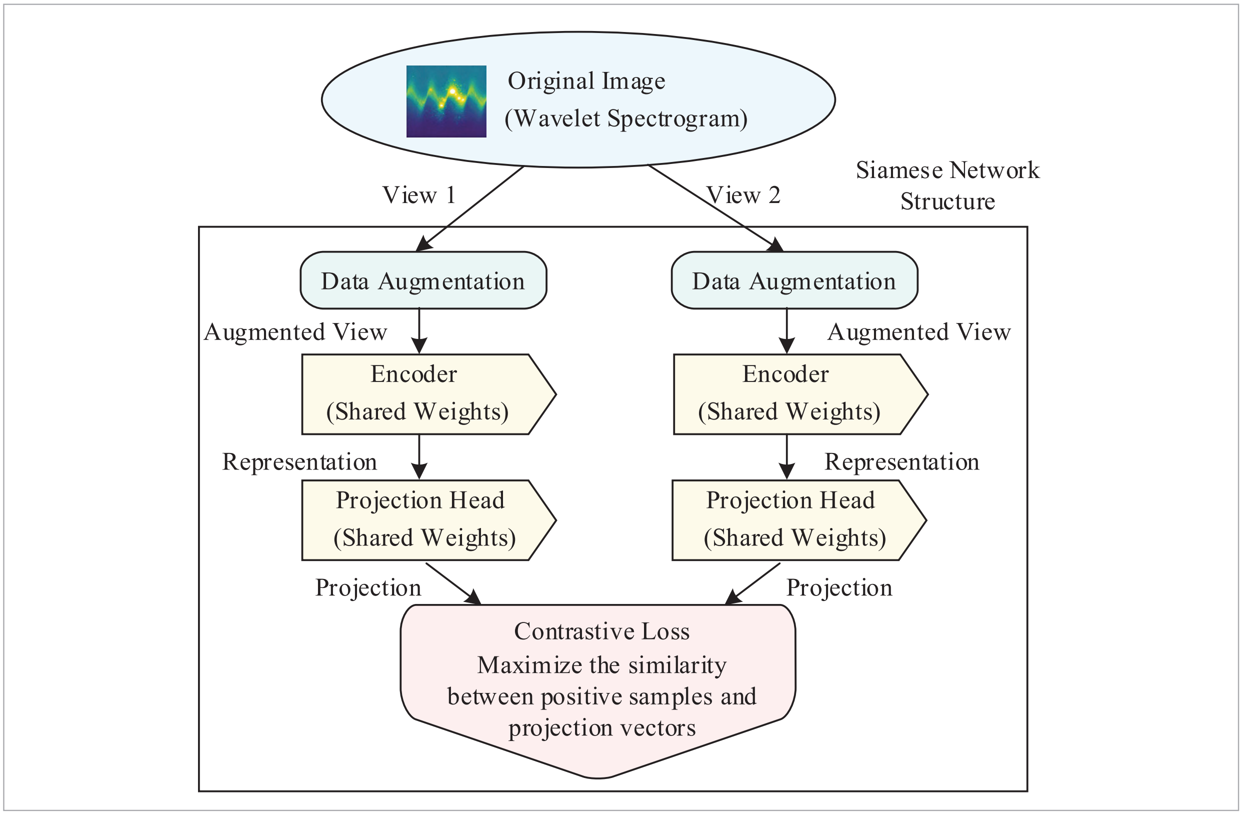

Figure 8
The overall architecture of a DIHAF.

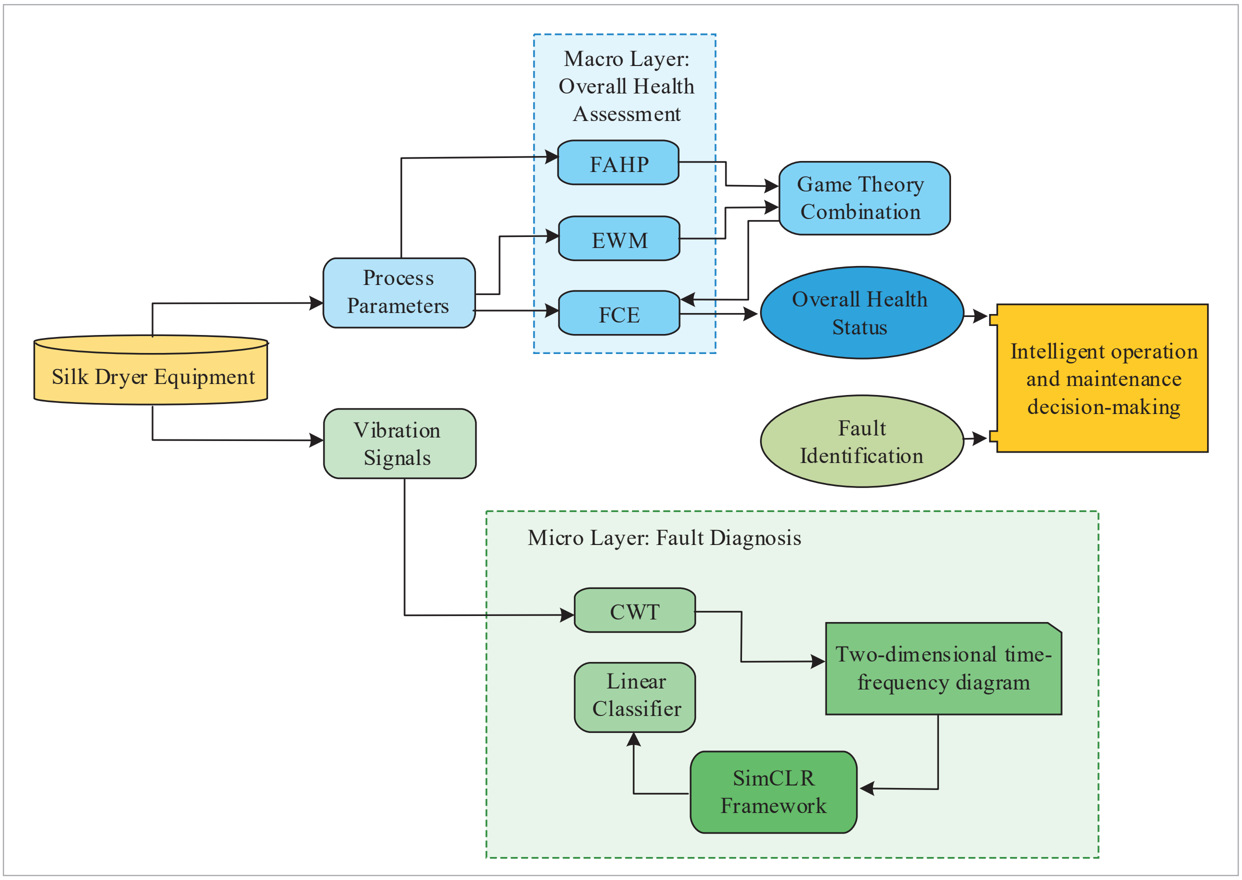

end evaluation process, the overall architecture of the DIHAF is shown in Figure 8. This framework consists of two parallel processing paths, with the upper layer being the macro evaluation layer. It utilizes process parameters and integrates FAHP and EWM weights through game theory to output the overall health status of the device. The lower layer is the micro-diagnosis layer, which uses vibration signals to identify fault types of specific components through CWT and SimCLR algorithms. The results of the two layers ultimately converge to jointly support the formulation of intelligent operation and maintenance decisions.

3. Results

To validate the effectiveness of the DIHAF, this paper conducts experimental analysis on the macroscopic HSA model and microscopic FDMs. Firstly, based on the actual operational data of CFDM, the accuracy and dynamic adaptability of the proposed dynamic HSA model are verified by comparing its performance with various traditional evaluation models. Secondly, the diagnostic performance under different working conditions, noise, and variable load conditions is evaluated by comparing it with various classical supervised and deep learning models.

3.1. Experimental Analysis of Dynamic HSA Model

To verify the efficacy of the proposed dynamic HSA model based on the combination of FAHP, EWM, and game theory weighting, this study conducts comparative experiments using historical operating data and expert diagnostic records of the Proctor K-600FX drum thin plate tobacco dryer in a cigarette factory's silk processing workshop. The experimental data are sourced from the historical operation logs of the Proctor K-600FX silk dryer recorded by the workshop's distributed control system over the past year. The data collection frequency is 1Hz, covering key process parameters such as temperature, moisture content, and cylinder wall temperature. Based on the company's "Equipment Maintenance Manual" and on-site expert repair records, historical data are manually labeled into five levels: healthy, good, attentive, abnormal, and faulty. These 50 representative sets of complete operational cycle data are selected as test cases. The compared models include the traditional fixed weight AHP model (M1), variable weight AHP model (M2), and combined static-weight model (M3). The dynamic HSA model proposed is M4. This study quantifies the evaluation performance of various evaluation models under different device states, calculates the evaluation accuracy and number of misjudgments. Among them, the number of single state misjudgments = the number of test cases for the state × (1- the accuracy of the state evaluation). The test results are shown in Figure 9. M1 has a fixed weight and strong subjectivity, with an average accuracy of only 69.4% and a total of 15.3 misjudgments. The accuracy drops sharply in "abnormal" and "fault" states, highlighting the problem of misjudgments. After introducing dynamic mechanisms in M2, the average accuracy increases to 82.8% and the number of misjudgments decreases to 8.6. Although there is improvement, it does not completely overcome the limitations of subjective frameworks, and there are still 2.6 misjudgments in the "fault" state. M3, relying on game theory combination weighting, achieves an average accuracy of 86.2% and reduces the number of misjudgments to 6.9, demonstrating the superiority of combination weighting. However, due to the lack of dynamic correction in this method, the number of misjudgments during the critical stages of "attention" and "abnormality" is still higher than the model proposed in the study. The average accuracy of M4 is as high as 97.2%, with only 1.4 false positives, and the evaluation accuracy far exceeds other models. This result indicates that the model balances accuracy and stability in equipment state assessment.

To verify the dynamic adaptability of the model to changes in tobacco dryer operating conditions, this study focuses on testing the health status tracking accuracy during the transition from abnormal to fault states. The experiment uses evaluation accuracy and Mean Absolute Error (MAE) as evaluation metrics, as shown in Table 1. During the transition from abnormal to faulty state, the health status score of the research model is closest to the actual health status score, with an overall evaluation accuracy of 97.2%. The evaluation accuracy of Model 1 is only 69.4%. Meanwhile, the MAE of Model 4 is only 3.15, a decrease of 8.30 and 5.77 compared to Models 2 and 3. In summary, the proposed color temperature dynamic HSA model can effectively track the health status of equipment during the transition from tobacco dryer abnormality to fault, and has good dynamic adaptability to changes in operating conditions.

Figure 9

The evaluation accuracy and number of misjudgments of each model.

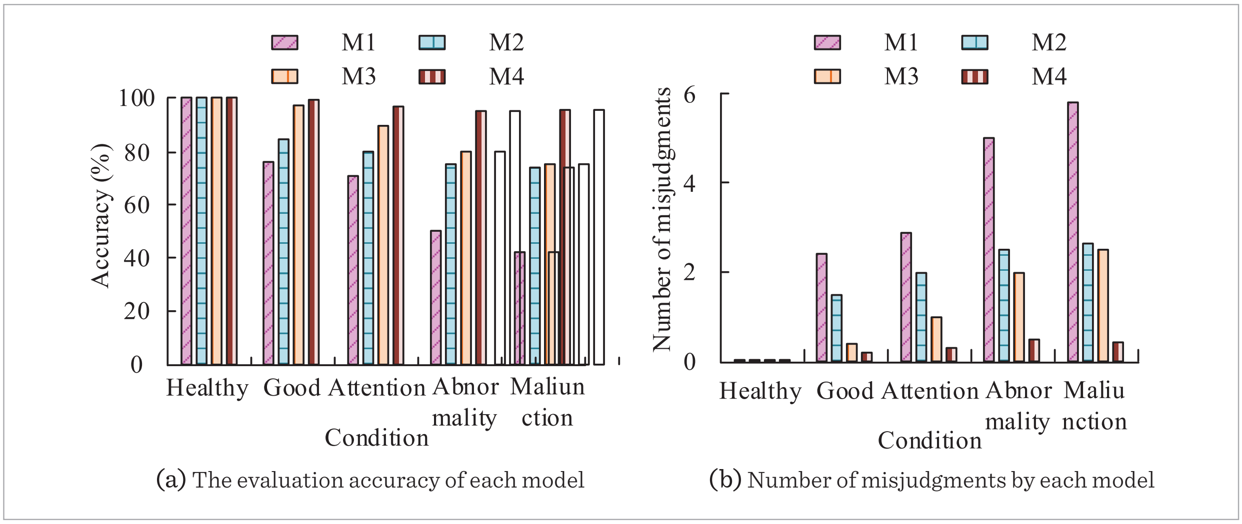

Table 1
Health score during the transition from abnormal to faulty state.

Point in time	Actual status of equipment	Actual Health score	M1	M2	M3	M4
T1	Attention	75	82	78	76	74
T2	Attention	72	75	76	76	73
T3	Attention	70	85	75	75	71
T4	In transition	67	81	72	75	68
T5	In transition	64	79	68	74	65
T6	In transition	61	76	65	74	62
T7	Enter Exception	58	72	60	73	58
T8	Abnormal	55	68	56	72	56
T9	Abnormal	53	71	54	71	54
T10	Abnormal	52	65	58	70	53
Accuracy			69.4%	82.8%	86.2%	97.2%
MAE			15.78	11.45	8.92	3.15

3.2. Experimental Analysis of UFD Using Wavelet Transform and SimCLR Fusion

To verify the performance of the proposed UFD method that combines wavelet transform and SimCLR, this study conducts experiments utilizing the internationally recognized Case Western Reserve University (CWRU) bearing fault dataset. This dataset consists of vibration signals collected by an accelerometer installed at the motor drive end, with a sampling frequency of 12 kHz. The experiment covers four different motor load conditions: 0HP, 1HP, 2HP, and 3HP. The fault modes include inner ring, outer ring, and rolling element damage, with three different fault diameters of 0.007, 0.014, and 0.021 inches for each type of damage, and a total of 10 health classifications, including normal state. In the data preprocessing stage, the sliding window method is used to slice the original signal, and the dataset is randomly divided into a training set and a testing set in an 8:2 ratio to verify the model's generalization ability. The environment is Ubuntu 20.04.4 LTS, based on Pytorch 1.18 deep learning framework. For performance comparison, this study selects two typical supervised models as benchmarks, including Support Vector Machine (SVM), the standard ResNet-18 with the same encoder structure as the research model, and Wide Deep Convolutional Neural Network (WDCNN). The settings of each model are listed in Table 2.

Table 2
Model settings.

Hyperparameter	Value
Learning Rate	0.001
Batch Size	256
Epoch	50
Distance Threshold	1.0

In the FDM that integrates wavelet transform and SimCLR, there is a key hyperparameter in the loss function, namely the temperature parameter τ, which is mainly responsible for adjusting the sensitivity of the model to negative samples. A smaller value of τ will sharpen the similarity distribution, making the model more focused on hard negative samples that are difficult to distinguish from positive samples, thereby increasing the penalty. On the contrary, larger values of τ will have a smooth distribution and treat all negative samples equally. To select the optimal value of τ, this study conducts a series of comparative experiments on the validation set, testing the final fault diagnosis accuracy and comparative loss values of the model after unsupervised pre-training when τ values are 0.05, 0.1, 0.2, 0.5, and 1.0. Figure 10 shows the convergence curves. In Figure 10(a), when the temperature parameter τ is 0.5, the convergence accuracy of the model is as high as 0.95. When τ=0.05 and τ=1.0, the convergence accuracy is only 0.83 and 0.86. In Figure 10(b), when the temperature parameter τ=0.5, the convergence loss value of the model is only 0.49, which is better than the other τ values. When the value of τ is 0.05, the convergence loss value is as high as 1.03, and the convergence epoch is the least, only 5 epochs. Therefore, the temperature parameter τ is ultimately selected as 0.5. Under this parameter, the model can achieve better fault diagnosis performance.

To visually demonstrate that the method of integrating wavelet transform and SimCLR can achieve similar samples being closer in the feature space and different samples being farther apart, this study uses the T-distributed random Neighbor Embedding (T-SNE) dimensionality reduction technique for visualization processing. The results are shown in Figure 11. Different colored circles represent samples of different categories. Figure 11(a) shows the T-SNE visualization results of the original test samples before training. Before training, the distribution of various types of data is relatively chaotic, with samples from different categories interwoven with each other and no obvious clustering trend. Figures 11(b)-(e) show the T-SNE visualization results of the test samples for the research model, SVM, ResNet-18, and WDCNN models after training. After training the research model, samples of the same class show a significant clustering and overlapping state, and the distance between samples of different classes increases significantly, causing an improvement in class discrimination. Although the test samples of the SVM model have a certain clustering tendency, there is still sample interweaving between some categories, and the category boundaries are not clear enough. Some categories of ResNet-18 samples are too close to distinguish. Although the samples trained by the WDCNN model have clustering effects, compared to the research model, the clustering density of similar samples and the distance between different samples are not as good. This result indicates that the clustering performance of the research model is superior to SVM, standard ResNet-18, and WDCNN models.

Further exploration is conducted on the fault detection accuracy and recall rates of various models under different noise environments. In Figure 12(a), the fault detection accuracy of all models shows an upward trend with the increase of Signal-to-Noise Ratio (SNR) values. When SNR=-4, the noise is the most severe, and the accuracy of the research model still reaches 90.2%, which is 24.9%, 14.6%, and 7.7% higher than SVM, ResNet-18, and WDCNN. As the SNR value increases from -4 to 8, the accu-

Figure 10

Convergence curve of experimental results.

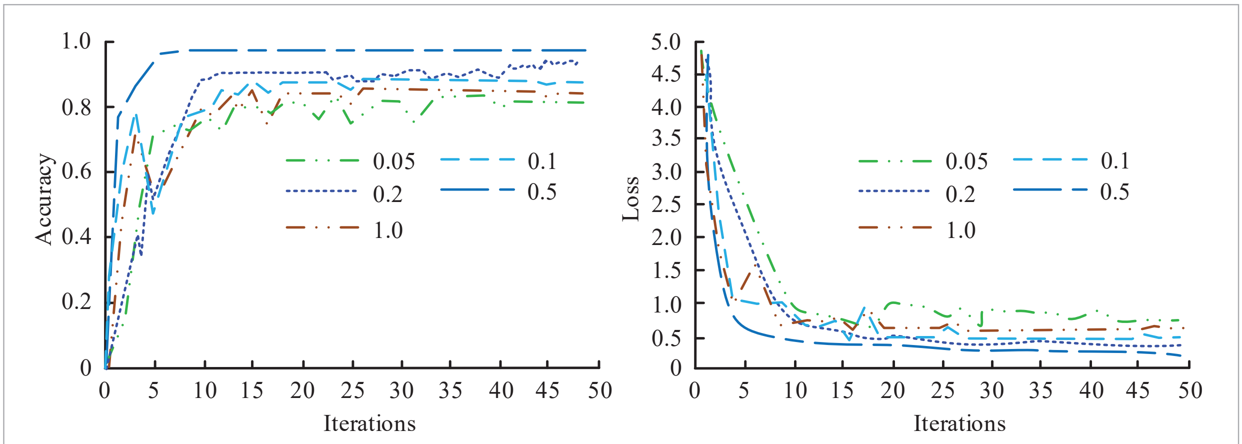

(a) Accurac (b) Loss

Figure 11

T-SNE visualization results.

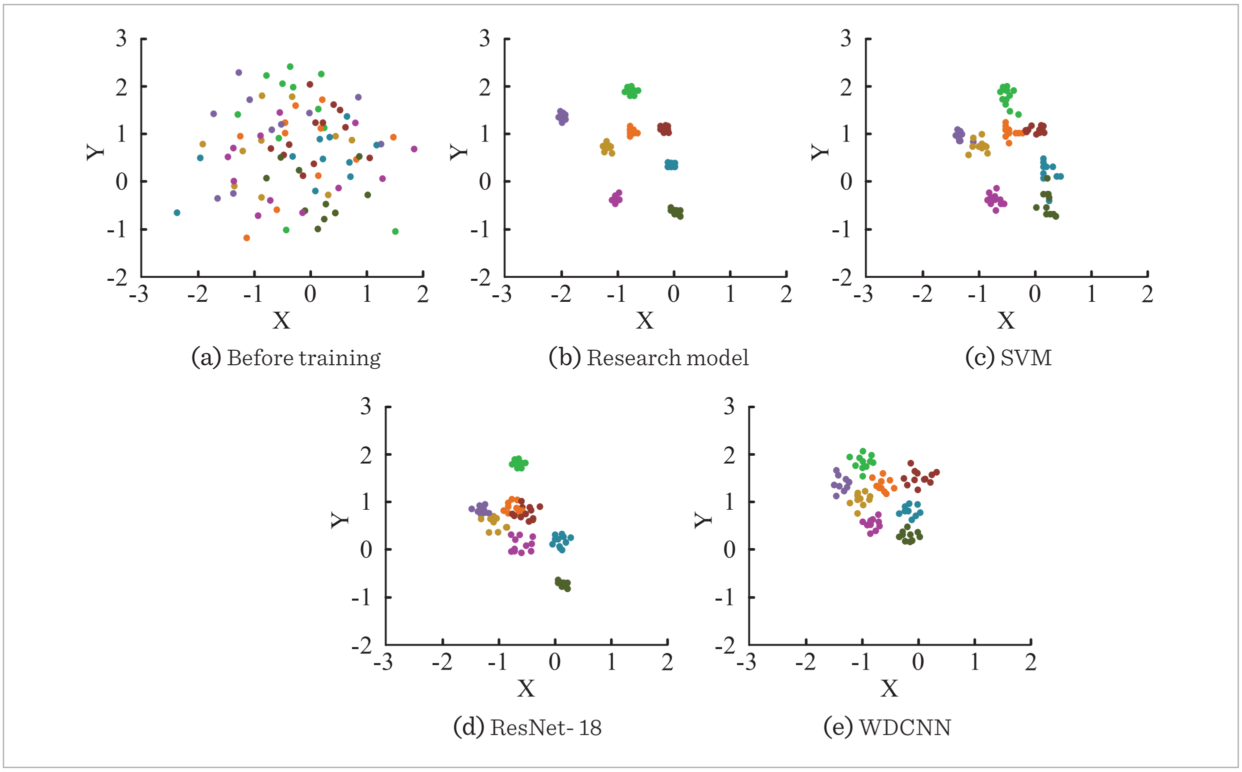

Figure 12

Accuracy and recall of fault detection under different noise environments.

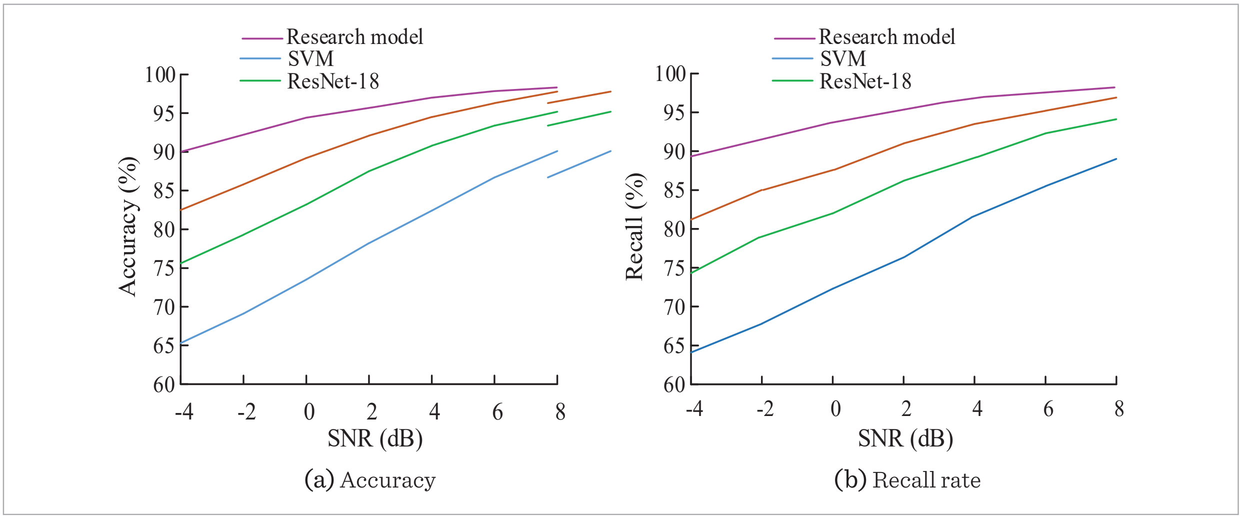

racy of the research model steadily increases from 90.2% to 98.5%, with an increase of 8.3% and smooth fluctuations. The accuracy of SVM has increased by 24.8%, while ResNet-18 and WDCNN models have increased by 19.6% and 15.3%, making them more sensitive to noise changes. In Figure 12(b), the recall rate of the research model consistently leads the comparison model. When SNR=-4, the recall rate of the model is 89.5%, far exceeding SVM's 64.1%, ResNet-18's 74.3%, and WDCNN's 81.2%. In a low-noise environment with SNR=8, the recall rate of this model is as high as 98.2%, which is 9.2% higher than SVM. This result indicates that the research model has high stability and reliability in fault detection under different noise environments.

In actual industrial production environments, the operating load of the tobacco dryer and other equipment often changes due to factors such as production batch and tobacco type. A robust fault diagnosis model should not only be effective under specific loads but also have the ability to generalize from training conditions to unknown conditions. Therefore, further exploration is conducted on the generalization performance of the research model under variable load conditions. The experiment will use 1HP, 2HP, and 3HP load data from the CWRU dataset for model training. The variable load conditions include 1HP → 2HP, 1HP → 3HP, 2HP → 3HP, 2HP → 1HP, 3HP → 1HP, 3HP → 2HP. Figure 13 shows the fault diagnosis, missed diagnosis rate, and misdiagnosis rate of each model under different variable load conditions. In Figure 13(a), the research model has the lowest missed diagnosis rate under all variable load conditions, and the values remain stable in the range of 1.9%-2.7%, with a fluctuation amplitude of only 0.8%. In contrast, SVM has the highest missed diagnosis rate, fluctuating within the range of 11.5%-15.2%, with a missed diagnosis rate of 15.2% in the

Figure 13

The missed diagnosis rate and misdiagnosis rate of each model's fault diagnosis.

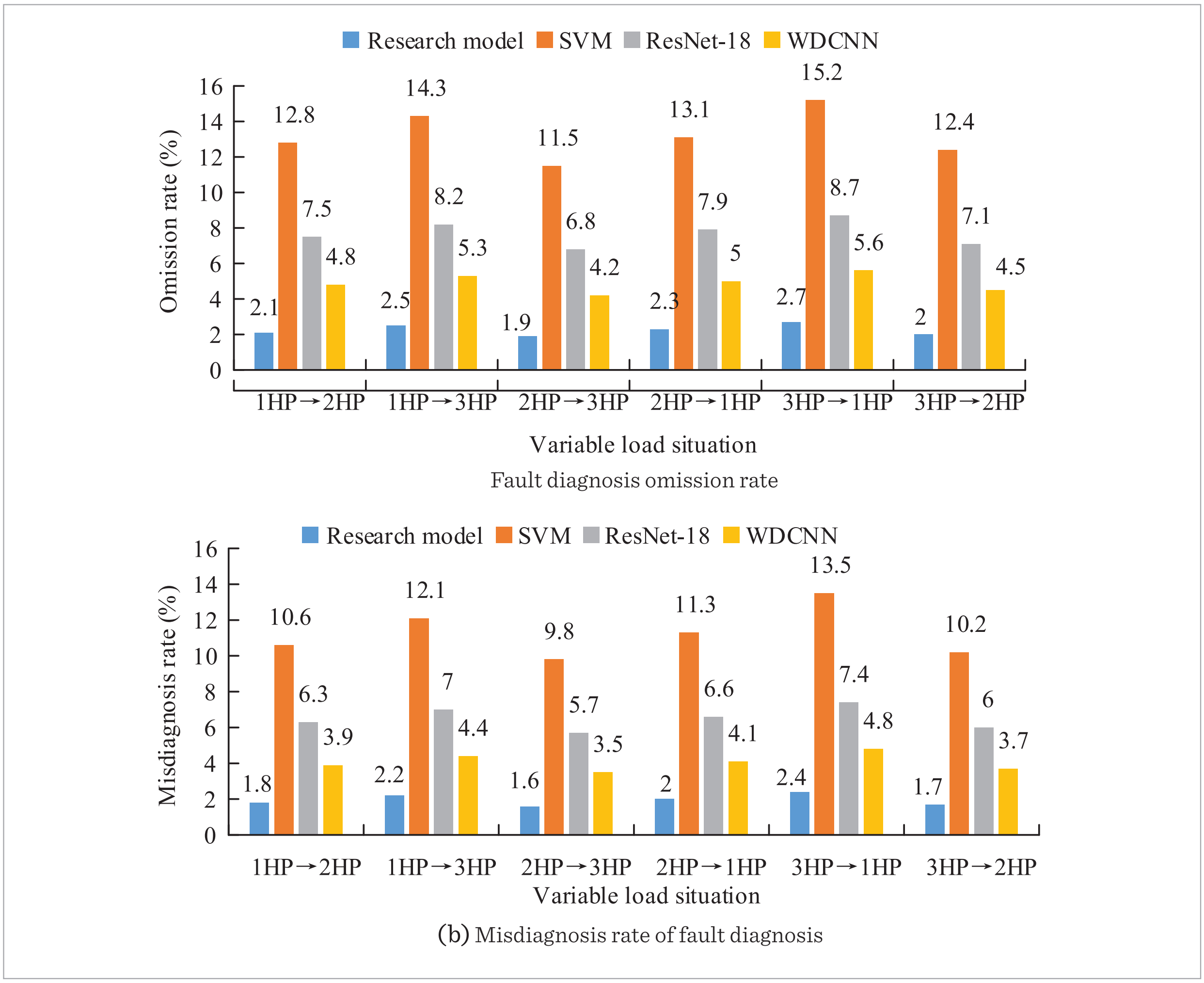

Table 3
The average accuracy, recall, F1-Score, and computational cost of each model on the test set.

Model	Accuracy (%)	Recall (%)	F1-Score (%)	Training Time (s/epoch)	Inference Time (ms/sample)
SVM	88.5	88.2	88.0	12.5	3.2
ResNet-18	91.1	91.3	91.0	45.6	14.5
WDCNN	93.5	93.8	93.4	38.2	10.2
Research model	97.2	97.4	97.2	48.3	11.8

3HP → 1HP variable load scenario. The missed diagnosis rates of ResNet-18 and WDCNN are between the two, ranging from 6.8% to 8.7% and 4.2% to 5.6%, and both increase significantly with the increase of variable load span. In Figure 13(b), the lowest misdiagnosis rate of the research model is only 1.6%, and the highest is only 2.4%. Among them, the misdiagnosis rate is the lowest in the 2HP → 3HP variable load scenario, and the highest in the 3HP → 1HP scenario, with outstanding overall stability. The misdiagnosis rate of SVM is still the highest, ranging from 9.8% to 13.5%. Its misdiagnosis rate under 3HP → 1HP is as high as 13.5%, which can easily lead to the misjudgment of normal equipment as a fault and increase unnecessary downtime costs. Although the misdiagnosis rates of ResNet-18 and WDCNN are lower than SVM, they are still higher than the research model, and their misdiagnosis rates fluctuate by 1.7% and 1.3% in variable load scenarios, both of which are higher than the research model. In summary, the fault diagnosis model integrating wavelet transform and SimCLR can effectively control the risk of missed diagnosis and misdiagnosis under variable load conditions, and its generalization performance is better than that of better adapting to the dynamic load changes of equipment, such as tobacco dryers in industrial scenarios.

To quantitatively evaluate the comprehensive performance of each model, Table 3 provides a detailed list of the average accuracy, recall, F1-Score, and computational cost of each model on the test set. According to Table 3, although the SVM model has an advantage in computational cost with an inference time of only 3.2 ms, its diagnostic indicators are the lowest, making it difficult to meet high-precision diagnostic requirements. The standard ResNet-18 model, due to its deep network layers, has a maximum inference time of 14.5 ms and an accuracy of 91.1%. The WDCNN model has achieved a good balance between efficiency and accuracy. In contrast, the proposed model performs the best in all performance indicators, with an average accuracy of 97.2% and an F1-Score of 97.1%. Due to the existence of the pre-training stage, the training time is slightly higher than that of WDCNN. However, in the inference stage that is most concerned with practical applications, thanks to the lightweight classifier structure after freezing the encoder, its single-sample inference time is only 11.8 ms. This result indicates that the model has good real-time processing capability while ensuring industry-leading diagnostic accuracy.

4. Discussion

To achieve effective HSA and fault diagnosis of CFDM equipment, this study constructed a DIHAF. In terms of macro HSA, a dynamic evaluation model integrating FAHP, EWM, and game theory has been proposed. The average evaluation accuracy of this model was as high as 97.2%, with a MAE of only 3.15, which was superior to traditional fixed weight, variable weight, and static combination weight models. This result was consistent with the conclusion of Rostami et al. that combination weighting can enhance the reliability of evaluation [6, 18]. The key to the better performance of the research model lay in the use of FAHP instead of traditional AHP, which better handled the ambiguity and uncertainty in expert judgment by introducing triangular fuzzy numbers, making subjective weights more realistic. Secondly, game theory was introduced to optimize the combination of subjective weights in FAHP and objective weights in EWM. Traditional combination weighting often used simple linear weighting, while game theory could find a Nash equilibrium point that minimizes the conflict between subjective expert knowledge and objective data information.

In terms of micro-level UFD, the T-SNE visualization results showed clear intra-class aggregation and inter-class separation in the trained features of the model that integrates CWT and SimCLR, compared to the mixed feature distribution generated by the original data and other models. This was mainly due to the signal processing capability of CWT, which converted 1D temporal vibration signals into more informative 2DTF maps, which can enhance feature extraction capabilities. Meanwhile, the contrastive learning mechanism of the SimCLR framework constructed a highly separable feature space by maximizing the consistency between different enhanced views of the same samples and minimizing the consistency with other samples. In terms of noise resistance and adaptability to variable loads, the research model maintained an accuracy of 90.2% even under strong noise with an SNR of -4, far exceeding the comparison models. Under different fixed loads, the accuracy remained stable at over 95.5%. This was consistent with the research conclusion of Rani et al. that SSL could improve the performance of models in small sample and complex operating conditions [17]. Among them, the self-supervised pre-training process utilized massive unlabeled data and diverse data augmentation, making the feature representations learned by the model have good invariance. Data augmentation simulated the noise and small changes in real working conditions, while the objective function of contrastive learning drove the model to ignore these interferences. Therefore, the research model learned about the characteristic representation of the nature of the fault, rather than just fitting the data representation under specific operating conditions. Specifically, the key reason why SSL based on SimCLR outperformed classical methods such as SVM and ResNet-18 was its effective utilization of data augmentation and feature invariance mechanisms. Traditional supervised learning models are prone to overfitting to noise patterns under specific operating conditions. SimCLR forces the model to learn the essential features of the image that remain unchanged after undergoing drastic transformations by applying random cropping, color distortion, and Gaussian blur enhancement operations to the time-frequency map. This mechanism enables the model to automatically ignore non-essential signal differences caused by background noise or load fluctuations, thereby extracting highly sensitive fault modes.

The improvement of the numerical performance of the model has important translational value in practical industrial applications. Firstly, the micro diagnostic model has an extremely low misdiagnosis rate in variable load and strong noise environments, which can significantly reduce unplanned downtime and ineffective manual troubleshooting costs caused by false alarms, directly reducing operation and maintenance expenses. Secondly, the high-precision tracking capability demonstrated by the macro model during the transition of equipment from anomalies to faults enables the operation and maintenance team to accurately perceive state degradation in the early latent stage of fault occurrence. This transformation helps optimize the development of maintenance plans and spare parts inventory management, avoiding resource waste caused by over-maintenance.

Although the proposed double-layer framework has demonstrated superior performance in the health assessment of tobacco dryers, there are still certain limitations. Firstly, in terms of applicability, current micro diagnosis only focuses on the single key component of rolling bearings, and has not yet covered other core components such as motor stator windings and gearbox gears. Subsequent research will focus on expanding the analysis framework and constructing a comprehensive diagnostic map that includes multi-component coupled faults. Secondly, in terms of computational cost, the pre-training process of the SimCLR model requires a large amount of computing resources, which limits its real-time deployment capability on resource-constrained industrial edge devices. Future research will explore lightweight techniques such as model pruning and quantization to reduce computational load. Finally, in terms of application depth, current research mainly focuses on state assessment and fault recognition. Future work will further explore the practical integration application of this framework in predictive maintenance systems to achieve a closed-loop from state perception to intelligent decision-making.

5. Conclusions and Recommendations

To enhance the intelligent operation and maintenance level of CFDM equipment, this study constructed a DIHAF that integrates macro HSA and micro fault diagnosis, including a dynamic HSA model based on game theory-optimized FAHP and EWM, and a UFD method combining CWT and SimCLR. The average evaluation accuracy of the dynamic HSA model was as high as 97.2%, with a total of only 1.4 false positives in 50 test cases. The average accuracy of the traditional weighted AHP model was the lowest, only 69.4%, with a total of 15.3 misjudgments. During the critical transition phase from "abnormal" to "faulty", the MAE between the predicted score and the actual value of the research model was only 3.15. The MAE of the variable weight AHP model was 11.45, and the MAE of the combined static weight model was 8.92. In the visualization results of T-SNE, the fault diagnosis model combining CWT and SimCLR could learn highly separable features from unlabeled data, and samples of different fault categories were compact within and separated between classes in the feature space. In the cross-condition test with variable load, the missed diagnosis rate of the research model remained stable within 1.9%-2.7%, and the misdiagnosis rate remained stable in the range of 1.6%-2.4%, with minimal fluctuations. Overall, the proposed DIHAF can achieve efficient HSA and fault diagnosis.

Conflicts of Interest

The author declares that there is no conflict of interest.

References

1. Chen, H., Luo, H., Huang, B., Jiang, B., Kaynak, O. Transfer Learning-Motivated Intelligent Fault Diagnosis Designs: A Survey, Insights, and Perspectives. IEEE Transactions on Neural Networks and Learning Systems, 2024, 35(3), 2969-2983. https://doi.org/10.1109/TNNLS.2023.3290974
2. Fırıldak, K., Çelik, G., Talu, M. F. SimCLR-Based Self-Supervised Learning Approach for Limited Brain MRI and Unlabeled Images. Bitlis Eren University Journal of Science, 2024, 13(4), 1304-1313. https://doi.org/10.17798/bitlisfen.1558069
3. Han, B., Tie, Y., Zhang, C., Zhang, Q., Zhang, S., Xu, X. Tunnel Lining Evaluation Based on A-EWM Cloud Model. Journal of Civil Structural Health Monitoring, 2025, 15(5), 1511-1528. https://doi.org/10.1007/s13349-024-00886-7
4. Hu, C., Wu, J., Sun, C., Yan, R., Chen, X. Interinstance and Intratemporal Self-Supervised Learning with Few Labeled Data for Fault Diagnosis. IEEE Transactions on Industrial Informatics, 2023, 19(5), 6502-6512. https://doi.org/10.1109/TII.2022.3183601
5. Hu, Y., Jia, Q., Yao, Y., Lee, Y., Lee, M., Wang, C., Yu, F. R. Industrial Internet of Things Intelligence Empowering Smart Manufacturing: A Literature Review. IEEE Internet of Things Journal, 2024, 11(11), 19143-19167. https://doi.org/10.1109/JIOT.2024.3367692
6. Imagawa, K., Shiomoto, K. Evaluation of Effectiveness of Self-Supervised Learning in Chest X-Ray Imaging to Reduce Annotated Images. Journal of Imaging Informatics in Medicine, 2024, 37(4), 1618-1624. https://doi.org/10.1007/s10278-024-00975-5
7. Kalibhat, N., Narang, K., Firooz, H., Sanjabi, M., Feizi, S. Measuring Self-Supervised Representation Quality for Downstream Classification Using Discriminative Features. Proceedings of the AAAI Conference on Artificial Intelligence, 2024, 38(12), 13031-13039. https://doi.org/10.1609/aaai.v38i12.29201
8. Lakhan, A., Hamouda, H., Abdulkareem, K. H., Alyahya, S., Mohammed, M. A. Digital Healthcare Framework for Patients with Disabilities Based on Deep Federated Learning Schemes. Computers in Biology and Medicine, 2024, 169, 107845. https://doi.org/10.1016/j.compbiomed.2023.107845
9. Li, G., Wang, J., He, J., Wang, J., Hou, T. FCE-Based Health Status Evaluation and IGM-Based Failure Prediction of Tool Magazine Manipulator for CNC

Machine Tools. Journal of Intelligent and Fuzzy Systems, 2024, 46(4), 10005-10018. https://doi.org/10.3233/JIFS-233028

10. Liu, X., Chen, Y., Wang, J., Chenshuang, A. N. G., Kehuan, L. U. O., Kehuan, W. A. N. G. Intelligent Fault Diagnosis Methods Toward Gas Turbine: A Review. Chinese Journal of Aeronautics, 2024, 37(4), 93-120. https://doi.org/10.1016/j.cja.2023.09.024

11. Liu, Y., Wang, M., Wang, Y. Location Decision of Emergency Medical Supply Distribution Centers Under Uncertain Environment. International Journal of Fuzzy Systems, 2024, 26(5), 1567-1603. https://doi.org/10.1007/s40815-024-01689-0

12. Lu, N., Zhou, W., Dou, Z. W. Can Intelligent Manufacturing Empower Manufacturing? An Empirical Study Considering Ambidextrous Capabilities. Industrial Management & Data Systems, 2023, 123(1), 188-203. https://doi.org/10.1108/IMDS-11-2021-0718

13. Ma, T., Wang, Z., Wu, D., Lu, P., Zhu, X., Yang, M., Wu, F. High-Areal-Capacity and Long-Cycle-Life All-Solid-State Battery Enabled by Freeze Drying Technology. Energy & Environmental Science, 2023, 16(5), 2142-2152. https://doi.org/10.1039/D3EE00420A

14. Mohammed, M. A., Abd Ghani, M. K., Lakhan, A., Al-Attar, B., Khaled, W. Federated Learning-Driven IoT and Edge Cloud Networks for Smart Wheelchair Systems in Assistive Robotics. Iraqi Journal for Computer Science and Mathematics, 2025, 6(1), 9. https://doi.org/10.52866/2788-7421.1241

15. Ozturk, S., Karipoglu, F. Investigation of the Best Possible Methods for Wind Turbine Blade Waste Management by Using GIS and FAHP: Turkey Case. Environmental Science and Pollution Research, 2023, 30(6), 15020-15033. https://doi.org/10.1007/s11356-022-23256-6

16. Pohan, F., Saputra, I., Tua, R. Scheduling Preventive Maintenance to Determine Maintenance Actions on Screw Press Machine. Journal Riset Ilmu Teknik, 2023, 1(1), 1-14. https://doi.org/10.59976/jurit.v1i1.4

17. Rani, V., Nabi, S. T., Kumar, M., Mittal, A., Kumar, K. Self-Supervised Learning: A Succinct Review. Archives of Computational Methods in Engineering, 2023, 30(4), 2761-2775. https://doi.org/10.1007/s11831-023-09884-2

18. Rostami, O., Tavakoli, M., Tajally, A. R., GhanavatiNejad, M. A Goal Programming-Based Fuzzy Best-Worst Method for the Viable Supplier Selection Problem: A Case Study. Soft Computing, 2023, 27(6), 2827-2852. https://doi.org/10.1007/s00500-022-07572-0

19. Shang, L., Zhang, Z., Tang, F., Cao, Q., Pan, H., Lin, Z. Signal Process of Ultrasonic Guided Wave for Damage Detection of Localized Defects in Plates: From Shallow Learning to Deep Learning. Journal of Data Science and Intelligent Systems, 2025, 3(2), 149-164. https://doi.org/10.47852/bonviewJDSIS32021771

20. Shi, L., Fu, S., Han, J., Liu, T., Zhan, S., Wang, C. The Mine Emergency Management Capability Based on EWM-CNN Comprehensive Evaluation. Engineering Management Journal, 2024, 36(3), 289-299. https://doi.org/10.1080/10429247.2023.2264162

21. Tashakori, A., Jiang, Z., Servati, A., Soltanian, S., Narayana, H., Le, K., Servati, P. Capturing Complex Hand Movements and Object Interactions Using Machine Learning-Powered Stretchable Smart Textile Gloves. Nature Machine Intelligence, 2024, 6(1), 106-118. https://doi.org/10.1038/s42256-023-00780-9

22. Tejani, G. G., Sadaghat, B., Kumar, S. Predict the Maximum Dry Density of Soil Based on Individual and Hybrid Methods of Machine Learning. Advances in Engineering Intelligent Systems, 2023, 2(3), 95-106. DOI: https://doi.org/10.22034/AEIS.2023.414188.1129

23. Wang, Y., He, P. Comparisons Between Fast Algorithms for the Continuous Wavelet Transform and Applications in Cosmology: The 1D Case. RAS Techniques and Instruments, 2023, 2(1), 307-323. https://doi.org/10.1093/rasti/rzad020

24. Wang, Y., Zhang, Y., Jiang, Z., Zheng, L., Chen, J., Lu, J. Prototype-Based Supervised Contrastive Learning Method for Noisy Label Correction in Tire Defect Detection. IEEE Sensors Journal, 2024, 24(1), 660-670. https://doi.org/10.1109/JSEN.2023.3336009

25. Więckowski, J., Sałabun, W., Kizielewicz, B., Bączkiewicz, A., Shekhovtsov, A., Paradowski, B., Wątróbski, J. Recent Advances in Multi-Criteria Decision Analysis: A Comprehensive Review of Applications and Trends. International Journal of Knowledge-Based and Intelligent Engineering Systems, 2023, 27(4), 367-393. https://doi.org/10.3233/KES-230487

26. Wu, J., Cabrera, D., Cerrada, M., Sánchez, R.-V., Sancho, F., Estupinan, E. Fault Diagnosis Generalization Improvement Through Contrastive Learning for a Multistage Centrifugal Pump. IEEE Transactions

on Reliability, 2025, 74(1), 2373-2381. https://doi.org/10.1109/TR.2024.3381014

27. Xu, W., Han, P., Proverbs, D. A New Approach to Evaluating Urban Flood Risk: The Case of Guangdong Province in China. Urban Water Journal, 2025, 22(4), 419-435. https://doi.org/10.1080/1573062X.2025.2472344

28. Zhang, D., You, Y., Liu, X. Study of EWM-Based Project Schedule Management in Tobacco Redrying Plants. Journal of Computational Methods in Sciences and Engineering, 2024, 24(6), 4065-4079. https://doi.org/10.1177/14727978241300053

29. Zhang, W., Chen, D., Xiao, Y., Yin, H. Semi-Supervised Contrast Learning Based on Multiscale Attention and Multitarget Contrast Learning for Bearing Fault Diagnosis. IEEE Transactions on Industrial Informatics, 2023, 19(10), 10056-10068. https://doi.org/10.1109/TII.2023.3233960

30. Zhang, Y., Liu, Z., Huang, Q. A Contrastive Learning-Based Fault Diagnosis Method for Rotating Machinery with Limited and Imbalanced Labels. IEEE Sensors Journal, 2023, 23(14), 16402-16412. https://doi.org/10.1109/JSEN.2023.3284044